ACS Sustainable Chemistry & Engineering

Research Article

pubs.acs.org/journal/ascecg

Reinforced and Ultraviolet Resistant Silks from Silkworms Fed with Titanium Dioxide Nanoparticles

Lingyue Cai, Huili Shao, Xuechao Hu, and Yaopeng Zhang*

State Key Laboratory for Modification of Chemical Fibers and Polymer Materials, College of Materials Science and Engineering, Donghua University, Shanghai 201620, China

Supporting Information

ABSTRACT: As the perfect combination of strength and luster, silkworm silks have been widely used in many fields but still need improvements. This paper demonstrates an *in vivo* uptake of titanium dioxide (TiO_2) nanoparticles by silkworms, leading to the direct production of intrinsically modified silk. The nanoparticles can be easily incorporated into the silk gland of silkworm by using this method due to the interactions between TiO_2 and silk fibroin molecules. Infrared spectra indicate that TiO_2 nanoparticles confine the conformation transition of silk fibroin from random coil/α-helix to β-sheet. Results of synchrotron radiation wide-angle X-ray diffraction and small-angle X-ray scattering suggest that modified silks have lower crystallinity, higher mesophase content, and higher Herman's orientation functions of crystalline region and mesophase region than control group. The breaking strength and elongation at break of the modified silk can be improved up to 548 ± 33 MPa and 16.7 ± 0.8%, respectively, by adding 1% nanoanatase into the artificial diet. Moreover, the TiO_2-1% modified silk shows well-improved ultraviolet resistant property as the breaking strength only decreased 15.9% after exposure to ultraviolet light for 3 h. The *in vivo* modification method for silkworm silk is a green, sustainable, and promising route for commercial production in the future.

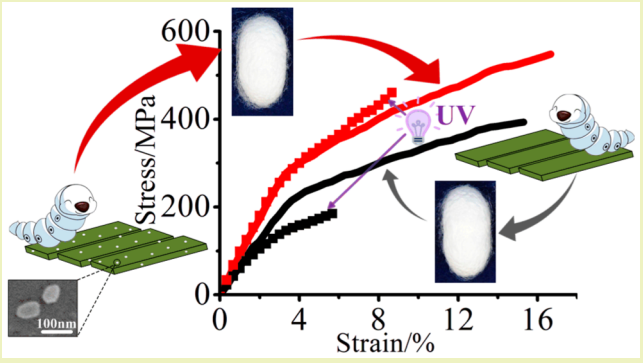

KEYWORDS: *Silkworm silk, TiO_2, Feeding method, Modification, Artificial diet*

INTRODUCTION

Silkworm silks, produced by silkworms from an aqueous circumstance, are fibrous proteins composed of fibroin and sericin.[1,2] They have been generally used in the textile industry and biomedical field for hundreds of year owing to their biocompatibility, controllable biodegradability, and excellent mechanical properties.[3−5] Silkworm silk easily rivals many synthetic fibers, but it still needs to be improved compared with spider dragline silk, another natural fiber, which embodies great strength and extensibility.[6] Many studies have focused on the improvement of its performance to make it rival or even exceed spider silks, as spider dragline silk cannot be easily obtained by domestic raising like silkworm silk.[7−11]

Silkworm silk can be modified because of its amino acid side chains.[12] Studies have proved that metallic elements could enhance mechanical properties of certain parts of organisms by incorporating into their inner structures, possibly forming some chelation.[13−18] Lee et al. integrated zinc, aluminum, or Ti into spider dragline silks by atomic layer deposition resulting in greatly increased toughness of the modified spider silks, which could be considered as a model for other biomaterials.[19] Recently, Pan et al. demonstrated that titanium dioxide (TiO_2) improved the toughness of artificial silk spun from regenerated silk fibroin solution.[11] Dickerson and Li found that TiO_2 with ultraviolet resistant property can attach to silks along with the oxide's chemical assembly onto a silk substrate.[20,21]

Meanwhile, researchers have devoted to finding out a proper way to incorporate some xenobiotics, such as metallic compounds[11,19,21−23] and dyes,[24−26] into silkworm silk by immobilizing the additive on the surface of silk or intercalating the additive into the silk. A typical example of the former is the silk dyeing industry, which consumes much resources and causes serious pollution.[27] For the latter, most experimenters add xenobiotics into silk fibroin solution and anew spin into silk. The process is long, complicated, and difficult to control.[11] However, Tansil et al. confirmed that dyes showed up in silk when silkworms were fed with a dye-containing diet.[28−30] Subsequently, Nisal et al. attained colored cocoons by adding azo dyes into feed of silkworms.[24] Recently, Teramoto and Kojima successfully incorporated phenylalanine (Phe) analogues into silk fibroin by simply adding azido-Phe to the diet of transgenic silkworms.[31] As the feeding method maintains the merit of natural silks and can easily get intrinsically modified silks, it is promising to produce high performance and functional silks on a large scale.

Received: July 24, 2015
Revised: August 26, 2015
Published: September 7, 2015

DOI: 10.1021/acssuschemeng.5b00749
ACS Sustainable Chem. Eng. 2015, 3, 2551−2557

In this work, silkworms were fed by artificial diet mixed with TiO_2 nanoparticles to improve the mechanical properties of silkworm silk. Moreover, the ultraviolet resistant property of the silk was also expected to be enhanced due to the ultraviolet-absorbing ability of TiO_2 nanoparticles. The effect of concentration gradient of the nanoparticles on the silk properties was also investigated.

MATERIALS AND METHODS

Preparation of Artificial Diet. The nano-TiO_2 solution (20 wt %, Hangzhou Wanjing New Material Co., Ltd., China) with different TiO_2 contents of 0.5, 1, 1.5 and 2 g was mixed with 100 mL of water, respectively. The size of the nano-TiO_2 ranged from 50 to 400 nm. Uniform dispersed nano-TiO_2 solutions were prepared by ultrasonic treatment for 15−20 min. Fifty grams of dry powder artificial silkworm diet was mixed with the diluted solution uniformly, and the mixture was microwaved for 3 min. The mass fraction ratio of TiO_2/dry diet powder was calculated as 1%, 2%, 3%, and 4%. The cooked artificial diet was pressed to be wafer for further feeding. The normal diet without adding TiO_2 solution was also processed for comparison.

The artificial silkworm diet was purchased from Shangdong Sericultural Research Institute, China. The ingredients of the diet include mulberry leaf powder (38.4%), defatted soybean powder (36.9%), corn powder (9.0%), green branches and petioles powder (5.0%), agar powder (5.0%) as well as bits of vitamin B complex, vitamin C, citric acid, and choline chloride.

Silkworm Raising. *Bombyx mori* silkworms were raised from eggs in a climatic chamber (Bilon HWS-350, Shanghai, China). The temperature and humidity were adjusted with the growth period of silkworms as listed in Table 1. One silkworm needs *circa* 2.5 g of artificial diet (dry weight) from its hatch to the first day of its fifth instar and *circa* 3 g of artificial diet (dry weight) with TiO_2 additive from the second day of its fifth instar to the start of fiber spinning. The silkworms were raised in boxes with breathable mesh. The boxes, with a size of 39 cm × 20 cm × 5 cm, can accommodate about 50 fifth instar silkworm larvae. A box of silkworms was raised for each group.

Table 1. Temperature and Relative Humidity of Silkworms in Different Growth periods

growth period of silkworms	temperature (°C)	relative humidity (%)
hatching	28	95
first instar	27	85
second instar	27	85
third instar	25	80
fourth instar	23	65
fifth instar	23	65

The silkworm larvae were fed with normal diet from their hatch to the first day of their fifth instar. Then, they were separated into five groups. Four groups were fed with modified diet and the other was fed with normal diet as control until their spinning.

Cocoon Degumming. Cocoons were dried for 1 h at 110 °C and 3 h at 80 °C in a vacuum drying oven. The dried cocoons were peeled into pieces and treated three times with 0.5 wt % aqueous Na_2CO_3 solution at 100 °C for 30 min, washed by deionized water, and naturally dried to get degummed silks. The samples were designated as TiO_2-*x* (*x* indicates the mass fraction ratio of TiO_2/dry diet powder). Silks from silkworms fed with normal diet were designated as control sample.

Characterization. Scanning electron microscopy (SEM) images were observed using a SEM (Hitachi S-3000N) instrument at 10 kV. The diameter of silks was measured by an optical microscope (BX-51, Olympus, Japan). For each sample, at least 20 single fibers were measured. As the cross section of the degummed cocoon silk is irregular, the accuracy of the diameter measurement was confirmed by comparing the optical microscopy method and typical weight/length method. Details can be found in the Supporting Information. Synchrotron radiation wide-angle X-ray diffraction (SR-WAXD) and synchrotron radiation small-angle X-ray scattering (SR-SAXS) patterns were obtained at the BL15U1 and BL16B1 beamlines at the Shanghai Synchrotron Radiation Facility (SSRF), respectively. For SR-WAXD, the wavelength (λ) and the spot size of the X-ray were 0.077 46 nm and 3 μm × 2 μm, respectively. For SR-SAXS, the λ and the spot size of the X-ray were 0.124 nm and 1 mm × 1 mm, respectively. FIT2D (V12.077) and Peakfit (V4.12) software were applied to process the patterns. Infrared spectra were recorded with a Nicolet 6700 (Thermo Fisher, USA) with a resolution of 0.09 cm^{-1} at 25 °C and 50% relative humidity. A diamond attenuated total reflectance (ATR) accessory was employed for the infrared spectra measurement. Quantitative analysis of the secondary structure was carried out by performing deconvolution of the spectra. The mechanical properties of the fibers (sample number 20) were measured with an Instron 5565 material testing instrument at 25 ± 2 °C and 50 ± 5% relative humidity. The experiment was performed at an extension rate of 2 mm min^{-1} with a gauge length of 10 mm. Ultraviolet resistant property of the TiO_2 modified silks was investigated by comparing the loss of the mechanical properties of the fiber after irradiation with ultraviolet light. The degummed silks were exposed to ultraviolet light at a wavelength of 390 nm and an intensity of 1245 $\mu W/cm^2$ for 3 h in a Rayven UV oven (Intelli-Ray 400, Uvitron) before tensile testing. Certain masses of degummed silk of control, TiO_2-1%, and TiO_2-2% silks were weighed and dissolved in 1 mL of concentrated nitric acid (65−68%). The solutions were then diluted 1000 times and subjected to ultrasonic treatment for 30 min. The content of Ti in the solutions was measured with an inductively coupled plasma mass spectrometry (ICP-MS) (NexIon 300x, PerkinElmer) to calculate the Ti content in the silk fibroin fibers.

RESULTS AND DISCUSSION

Effect of TiO_2 Content in the Artificial Diet on Growth and Silk of Silkworms. Figure 1a shows the photos of the silkworms and cocoons as well as the SEM images of the degummed silks, and the diameters of the fibers are listed in Table 2 (the second column) for comparison. As shown in Figure 1a, the silkworms do not exhibit any difference. However, it was observed that the color of the silkworm excrement became shallow with increasing additive amount of TiO_2 in the process of the experiment. Therefore, it seems reasonable that most of the TiO_2 was discharged by silkworms. The size of the cocoons in each group is uniform, as shown in the third column of Figure 1a. Furthermore, the color, size, and configuration of the modified cocoons and control cocoons in Figure 1b almost have no differences. From the SEM images of Figure 1a, it can be seen that TiO_2 has limited influences on the silk fibers. No TiO_2 particles were observed on the surface of the silks. However, it is clear that the size of the cocoons from silkworms fed with artificial diet is relatively smaller than that of cocoons from mulberry silkworms. The diameter of the conventional silk obtained from the silkworms fed with mulberry was measured to be 11.7 ± 1.1 μm by the optical microscope, which is about 1 μm thicker than that of silks from silkworms fed with artificial diet as shown in Table 2. The artificial diet may not supply sufficient nutrition or taste for silkworms as mulberry leaves. Moreover, the artificial diet was dehydrating at the time of silkworm feeding and hardly to be cleaned. All these factors might result in the poor effect on the silkworm growth. In addition, TiO_2 nanoparticles were taken in by silkworms and spread into the silk gland. The interactions between the TiO_2 nanoparticles and silk fibroin may also affect the spinning behaviors of silkworms. Thus, the average diameter of the degummed silk presents a slightly downward trend along with increasing additive amount of TiO_2. It was observed that the TiO_2 added diet did not cause any reduction

DOI: 10.1021/acssuschemeng.5b00749
ACS Sustainable Chem. Eng. 2015, 3, 2551−2557

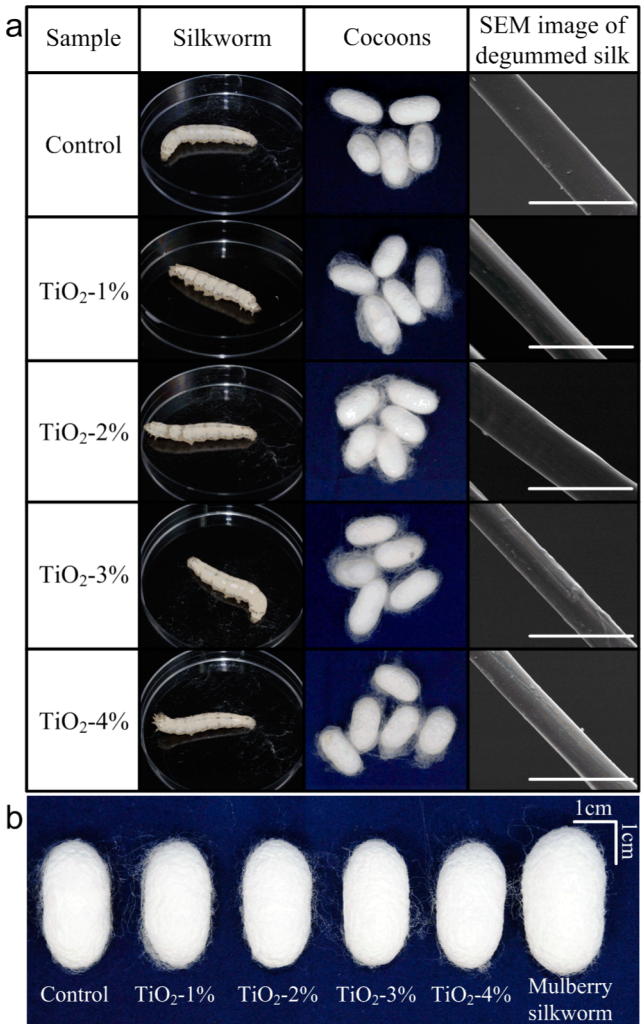

Figure 1. Effect of TiO_2 content in the artificial diet on (a) growth, cocoons, and degummed silk of silkworms. The silkworm in the culture dish with a diameter of 9 cm is in the fifth instar, and the scale bar shown in the SEM images of degummed silk is 30 μm. The images shown in panel b are the single cocoons of silkworms fed on artificial diet and mulberry, respectively.

of food intake or death of silkworms. The speed of food intake and the growth rate of silkworms also had no obvious difference in the five groups. In addition, Li et al. considered that the addition of TiO_2 nanoparticles could improve both protein and carbohydrate metabolisms of silkworms.[32] Therefore, we postulate that TiO_2 nanoparticles have no obvious toxicity to silkworms at a low content.

Secondary Structure of Degummed Silks. FTIR spectra of degummed silks are depicted in Figure 2a. TiO_2 does not change the basic structure of silkworm silks, which can be confirmed from the identical peak position of FTIR spectra. This paper employs general assignment of adsorption peaks in amide I band. The broad peak from 1655 to 1660 cm^{-1} is considered to be either the random coil or the helical conformation, or both; the peaks centered at 1620−1660 cm^{-1} and 1690−1700 cm^{-1} are classified as the β-sheet and β-turn conformations, respectively.[33−36] The deconvolution of FTIR spectra in amide I band of single degummed silks are shown in Figure S1. The secondary structure contents obtained by FTIR are shown in Figure 2b. It can be seen that the TiO_2 modified silks have higher random coil/α-helix content and lower β-sheet content than control silk. Moreover, the random coil/α-helix and β-sheet contents in the TiO_2 modified silks show upward and downward trend with increasing additive amount, respectively. Simultaneously, the β-turn contents of the TiO_2 modified silks are higher than that of control silk. A downward trend of β-turn content is exhibited with increasing additive amount. The structural characteristics of TiO_2 modified silks observed here might be attributed to the confined crystallization of silk fibroin induced by the nanoparticles.[11] In a word, TiO_2 hinders the conformation transition from random coil/α-helix to β-sheet of silk fibroin and higher content of TiO_2 leads to more evident confined crystallization effect.

Crystalline Structures, Orientation and Interface Structure analysis of TiO_2 Modified Silks. SR-WAXD was used to investigate the crystalline structures and orientation of silk fibers. Figure 3a,b show the 2D SR-WAXD patterns and 1D SR-WAXD patterns, and the deconvolution of the 1D SR-WAXD patterns are shown in Figure S2. The Herman's orientation functions and crystalline structural parameters obtained by WAXD are listed in Table 2. From Figure 3a,b, it can be found that both the 1D and 2D WAXD patterns do not show obvious differences. Here, it is essential and crucial to discuss the role of mesophase or called interface phase, which acts as a modulus intermediate between the amorphous and crystalline phase and is of great significance in affecting the mechanical properties of silk fibers.[37] The orientation functions and content of mesophase in this paper were calculated according to references.[38−41]

As shown in Table 2, the TiO_2 modified silks have lower crystallinity than the control silk, which is consistent with the FTIR results. The $f_{mesophase}$ and mesophase contents are higher in modified silks, whereas the $f_{crystal}$ is comparable. In addition, the orientation functions and crystallinity of the modified silks both show downward trends, whereas the mesophase content shows upward trends with increasing additive amount. Crystallite size of the degummed silks increases in the *a* direction (interchain direction) and *b* direction (intersheet direction) with increasing TiO_2 content. For the *c* direction (fiber axis), the TiO_2 modified silks have an obvious decrease compared with control silk. The variation of the crystallite size

Table 2. Average Diameter, Herman's Orientation Functions, and Crystalline Structural Parameters of the Degummed Silks

						crystallite size (nm)		
sample	average diameter (μm)	$f_{crystal}$	$f_{mesophase}$	crystallinity (%)	mesophase content (%)	L_a	L_b	L_c
control	10.9 ± 0.7	0.9736	0.8419	48.9	10.2	3.34	3.37	12.56
TiO_2-1%	10.6 ± 0.7	0.9759	0.8964	45.7	12.5	4.46	5.73	7.59
TiO_2-2%	10.5 ± 0.8	0.9751	0.8841	44.2	13.5	5.82	5.99	7.88
TiO_2-3%	10.5 ± 0.9	0.9709	0.8529	43.1	13.8	6.92	6.37	7.59
TiO_2-4%	10.4 ± 0.8	0.9697	0.8560	40.3	15.3	7.87	7.57	8.74

DOI: 10.1021/acssuschemeng.5b00749
ACS Sustainable Chem. Eng. 2015, 3, 2551−2557

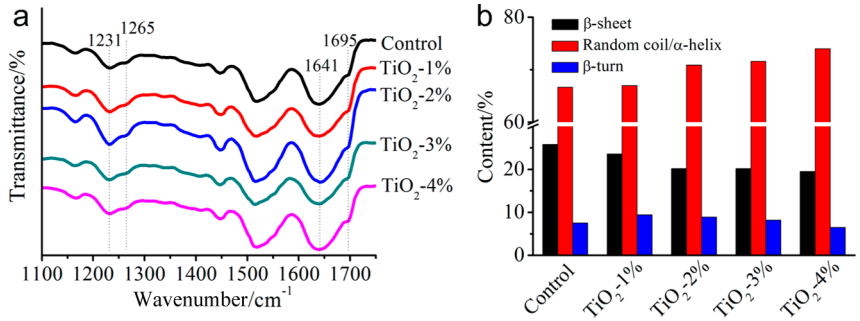

Figure 2. (a) FTIR spectra of degummed silks and (b) the deconvolution result of FTIR spectra in amide I band.

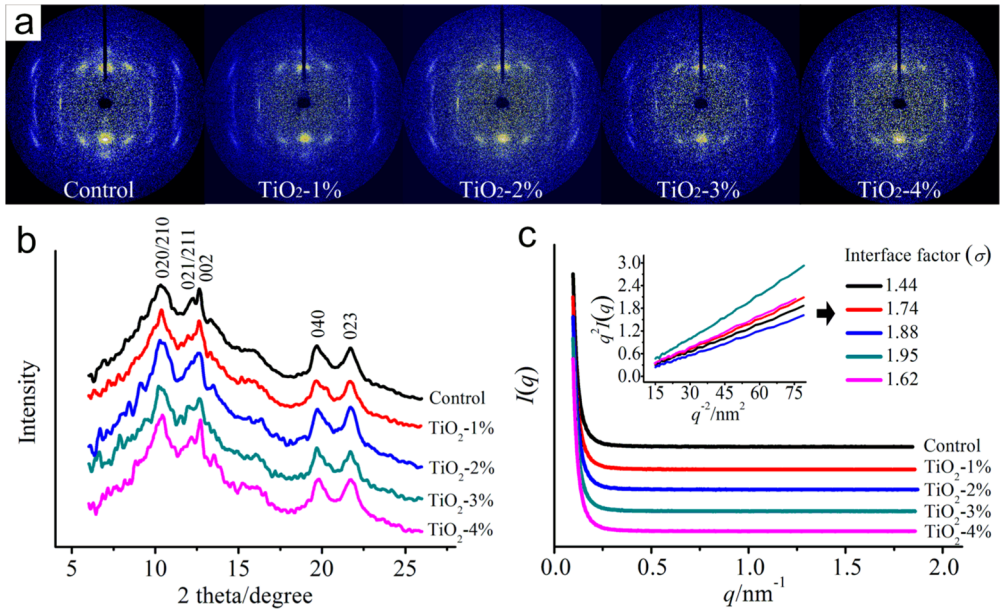

Figure 3. Crystalline structures and interface structure analysis of TiO_2 modified silks. (a) 2D, (b) 1D SR-WAXD patterns, and (c) SR-SAXS patterns of degummed silks. The inset in panel c is the $q^2I(q) - q^{-2}$ curve based on the modified Porod formula. $I(q)$ is the scattering intensity and q is the scattering vector. The interface parameter (σ) is listed in panel c.

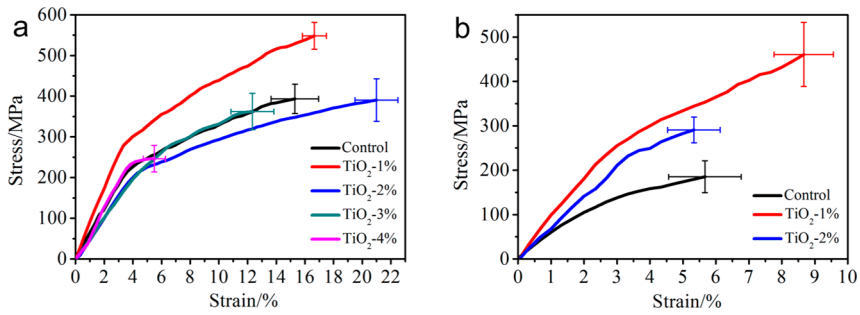

Figure 4. Stress−strain curves of (a) degummed silk and (b) degummed silk exposed to ultraviolet for 3 h.

in the c direction among the modified silks has no conspicuous regularity. Because silkworm silk forms an orthogonal crystallite, the crystalline volume can be evaluated as $L_a \times L_b \times L_c$, referring to references 42 and 43. The results suggest that the crystalline volume increases with increasing TiO_2 additive amount. As mentioned above, TiO_2 induced a confined crystallization of silk fibroin. Because TiO_2 nanoparticles interacted with the protein molecules and restricted the movement of protein molecules, it was difficult to increase the nucleation sites of crystallization for silk fibroin around TiO_2 nanoparticles. However, silk fibroin molecules could be free to crystallize in nonconfined regions, which decreased with increasing TiO_2 content. In the spinning process of silkworms, the silk fibroin in the nonconfined regions could form grains with bigger size under the same driving force of crystallization. Eventually, less crystalline structure but bigger grains were formed in the modified fibers.

Furthermore, the evidence for the mesophase in silkworm silks was also demonstrated by SR-SAXS. The 2D SR-SAXS patterns are illustrated in Figure S3. Figure 3c shows the 1D SAXS spectra of the silks and the inset is the profiles of $q^2I(q) - q^{-2}$ based on the modified Porod law, which was used to

DOI: 10.1021/acssuschemeng.5b00749
ACS Sustainable Chem. Eng. 2015, 3, 2551−2557

calculate the interface factor (σ). The thickness of interface was approximately calculated, and is listed in Table S1.[11,44−46] The results listed in the inset of Figure 3c suggest that the interface factors of the modified silks are larger than that of control silk. Since the interface factor is in direct proportion to the thickness of the interface, it is reasonable to consider that TiO_2 modified silks have a thicker interface than control silk. The thickness of interface increases with increasing TiO_2 additive amount below 3%. However, when the concentration increased to 4%, the thickness of the interface decreased a little, which might be attributed to the poorer combination between silk fibroin and agglomerated nano-TiO_2.

Mechanical Properties of Degummed Silks. The stress−strain curves of the degummed silks are shown in Figure 4a. It can be seen that TiO_2 has a remarkable influence on the mechanical properties of silks. TiO_2-1% silk exhibits a higher breaking strength of 548 ± 33 MPa, exceeding that of control silk (393 ± 36 MPa). The breaking strength of the TiO_2-2% silk is similar to the control, but the elongation at break is extended to 21.0 ± 1.5%. However, the modified silk becomes weaker when the additive amount of the nano-TiO_2 further increases to 3% and 4%.

The absorbed TiO_2 might not be transformed into some kinds of new form, as there is no possible chemical reaction between inert TiO_2 nanoparticles and silk fibroin. The above FTIR results also do not show any evidence of a new compound containing Ti. The most possible form for the Ti compounds in silk fiber is still TiO_2 nanoparticles. Pan et al. obtained tough artificial silk by adding TiO_2 into regenerated silk fibroin solution and put forward a nanoconfined crystallite toughening mechanism. They indicated that the coordination complexes and hydrogen bonds of TiO_2 and fibroin matrix confined the conformation transition from random coil/α-helix to β-sheet. As the nanoparticles act as knots in the fiber, forming a "cross-linked" network with the crystallites, lower crystallinity and higher breaking elongation were obtained.[11] This mechanism could also be applied to explain the decrease of β-sheet content and crystallinity of TiO_2 modified silks. The increase of amorphous region may result in higher breaking elongation of TiO_2-1% and TiO_2-2% silks. It is interesting that the $f_{mesophase}$ of the modified silks shows an increase instead of reduction like in Pan's work. This may contribute to the higher and comparable breaking strength of TiO_2-1% and TiO_2-2% silks, as the nanoparticles with low contents were well absorbed by silkworms. However, when the additive amount increases to 3% and 4%, the mechanical properties of the modified silks start getting poor. The high additive amount of TiO_2 is likely to exceed the absorbing capacity of the silkworms, and the agglomerating of nanoparticles at a high concentration may impede the combination of nanoparticles and silk fibroin. Thus, the $f_{mesophase}$ shows obvious decrease than TiO_2-1% and TiO_2-2% silks and closes to that of the control silk (Table 2). Moreover, the aggregations might act as defects instead of link points resulting in poorer mechanical properties of the modified silks, especially for TiO_2-4% silk.

Ultraviolet Resistant Properties of TiO_2 Modified Silks and Quantification of Ti in the Silk Fibroin. Ultraviolet resistant properties of TiO_2-3% and TiO_2-4% silks were not tested as the poorer mechanical properties than the control silk. The stress−strain curves of control, TiO_2-1%, and TiO_2-2% silks are plotted in Figure 4b. As expected, the breaking strength and the elongation at break of the ultraviolet irradiated silks were lower than those of the untreated silks, because the ultraviolet light may break protein chains. The control silk was weakened the most whereas TiO_2-1% silk kept the most of the mechanical properties.

As shown in Figure 4b, the breaking strengths of control, TiO_2-1%, and TiO_2-2% silks decreased 52.9%, 15.9%, and 25.4% (reduction of the average strength/original average strength), respectively. Therefore, the addition of the TiO_2 certainly improved the ultraviolet resistance of silkworm silk. In general, the ultraviolet resistance of the material may be enhanced with the increase content of TiO_2, but the tensile properties of TiO_2-2% silk decreased more than TiO_2-1% silk. This is because TiO_2-2% silk has more amorphous region which is easier to be damaged than crystalline region under ultraviolet light.

To make sure that the structure and property differences between the modified and control silks are resulted from the TiO_2, the content of Ti in the fibroin was quantified, and the results are listed in Table 3. As the mechanical properties of TiO_2-3% and TiO_2-4% silk were poorer than those of control silk, it is not necessary to measure the Ti content in the two silks.

Table 3. Content of Ti in Degummed Silk Fibers

sample	control	TiO_2-1%	TiO_2-2%
content (wt %)	2.27×10^{-4}	4.9×10^{-3}	2.05×10^{-2}

It should be mentioned that silk fiber itself contains a small amount of Ti. The amount of Ti in the control silk was detected to be 2.27×10^{-4}%. It is clear from Table 3 that the addition of TiO_2 results in the increased content of Ti in the silk fibroin part of silk fiber. Moreover, the content of Ti in silk fibroin fiber increases with the additive amount of TiO_2. Therefore, it can be concluded that a certain content of TiO_2 was absorbed by the silkworms and entered the silkworm gland. Meanwhile, most of the TiO_2 nanoparticles were excreted from the silkworm. It is uncertain whether TiO_2 nanoparticles were also incorporated in the sericin surrounding silk fibroin, as the sericin was removed during the degumming process of silkworm silk.

CONCLUSION

In this study, silks were modified by raising silkworms with a TiO_2-containing diet. It was found that TiO_2 influences the mechanical properties and ultraviolet resistant properties of silks. Compared with those of the control silk, the breaking strength of 548 ± 33 MPa and elongation of 16.7 ± 0.8% of the TiO_2-1% modified silk increased 39.2% and 8.9% on average, respectively. The breaking strength of TiO_2-1% silk decreased just 15.9% whereas that of control silk decreased 52.9% after exposure to ultraviolet light. However, both the breaking strength and ultraviolet resistant property were reduced when the content of TiO_2 was further increased. This feeding method can potentially apply to other metallic compounds for improving the performance of silks or effectively combining some novel functions with silks at low-costs. The functional silks with exceptional mechanical properties can be used for nonconventional textiles as well as tissue engineering.

DOI: 10.1021/acssuschemeng.5b00749
ACS Sustainable Chem. Eng. 2015, 3, 2551−2557

■ ASSOCIATED CONTENT

Supporting Information

The Supporting Information is available free of charge on the ACS Publications website at DOI: 10.1021/acssuschemeng.5b00749.

Comparison of silk cross-sectional area measured by weight/length method and optical microscopy, figures for 2D SR-SAXS as well as deconvolution of FTIR and SR-WAXD patterns, and table for interface thickness (PDF).

■ AUTHOR INFORMATION

Corresponding Author

*Y. Zhang. Fax: +86-21-67792955. Tel: +86-21-67792954. E-mail: zyp@dhu.edu.cn.

Notes

The authors declare no competing financial interest.

■ ACKNOWLEDGMENTS

This work is supported by the National Natural Science Foundation of China (21274018), DHU Distinguished Young Professor Program (A201302), the Fundamental Research Funds for the Central Universities (2232013A3-11), and the Programme of Introducing Talents of Discipline to Universities (No. 111-2-04).

■ REFERENCES

(1) Hakimi, O.; Knight, D. P.; Vollrath, F.; Vadgama, P. Spider and mulberry silkworm silks as compatible biomaterials. *Composites, Part B* **2007**, *38* (3), 324−337.

(2) Omenetto, F. G.; Kaplan, D. L. New Opportunities for an Ancient Material. *Science* **2010**, *329* (5991), 528−531.

(3) Rockwood, D. N.; Preda, R. C.; Yucel, T.; Wang, X. Q.; Lovett, M. L.; Kaplan, D. L. Materials fabrication from Bombyx mori silk fibroin. *Nat. Protoc.* **2011**, *6* (10), 1612−1631.

(4) Cao, Y.; Wang, B. C. Biodegradation of Silk Biomaterials. *Int. J. Mol. Sci.* **2009**, *10* (4), 1514−1524.

(5) Ude, A. U.; Eshkoor, R. A.; Zulkifili, R.; Ariffin, A. K.; Dzuraidah, A. W.; Azhari, C. H. Bombyx mori silk fibre and its composite: A review of contemporary developments. *Mater. Eng.* **2014**, *57*, 298−305.

(6) Vollrath, F.; Knight, D. P. Liquid crystalline spinning of spider silk. *Nature* **2001**, *410* (6828), 541−548.

(7) Teule, F.; Miao, Y. G.; Sohn, B. H.; Kim, Y. S.; Hull, J. J.; Fraser, M. J.; Lewis, R. V.; Jarvis, D. L. Silkworms transformed with chimeric silkworm/spider silk genes spin composite silk fibers with improved mechanical properties. *Proc. Natl. Acad. Sci. U. S. A.* **2012**, *109* (3), 923−928.

(8) Holland, C.; Terry, A. E.; Porter, D.; Vollrath, F. Natural and unnatural silks. *Polymer* **2007**, *48* (12), 3388−3392.

(9) Zhou, G. Q.; Shao, Z. Z.; Knight, D. P.; Yan, J. P.; Chen, X. Silk Fibers Extruded Artificially from Aqueous Solutions of Regenerated Bombyx mori Silk Fibroin are Tougher than their Natural Counterparts. *Adv. Mater.* **2009**, *21* (3), 366−370.

(10) Gandhi, M.; Yang, H.; Shor, L.; Ko, F. Post-spinning modification of electrospun nanofiber nanocomposite from Bombyx mori silk and carbon nanotubes. *Polymer* **2009**, *50* (8), 1918−1924.

(11) Pan, H.; Zhang, Y. P.; Shao, H. L.; Hu, X. C.; Li, X. H.; Tian, F.; Wang, J. Nanoconfined crystallites toughen artificial silk. *J. Mater. Chem. B* **2014**, *2* (10), 1408−1414.

(12) Vepari, C.; Kaplan, D. L. Silk as a biomaterial. *Prog. Polym. Sci.* **2007**, *32* (8−9), 991−1007.

(13) Lichtenegger, H. C.; Schoberl, T.; Ruokolainen, J. T.; Cross, J. O.; Heald, S. M.; Birkedal, H.; Waite, J. H.; Stucky, G. D. Zinc and mechanical prowess in the jaws of Nereis, a marine worm. *Proc. Natl. Acad. Sci. U. S. A.* **2003**, *100* (16), 9144−9149.

(14) Morgan, T. D.; Baker, P.; Kramer, K. J.; Basibuyuk, H. H.; Quicke, D. L. J. Metals in mandibles of stored product insects: do zinc and manganese enhance the ability of larvae to infest seeds? *J. Stored Prod. Res.* **2003**, *39* (1), 65−75.

(15) Broomell, C. C.; Mattoni, M. A.; Zok, F. W.; Waite, J. H. Critical role of zinc in hardening of Nereis jaws. *J. Exp. Biol.* **2006**, *209* (16), 3219−3225.

(16) Pontin, M. G.; Moses, D. N.; Waite, J. H.; Zok, F. W. A nonmineralized approach to abrasionresistant biomaterials. *Proc. Natl. Acad. Sci. U. S. A.* **2007**, *104* (34), 13559−13564.

(17) Cribb, B. W.; Stewart, A.; Huang, H.; Truss, R.; Noller, B.; Rasch, R.; Zalucki, M. P. Insect mandibles-comparative mechanical properties and links with metal incorporation. *Naturwissenschaften* **2007**, *95* (1), 17−23.

(18) Broomell, C. C.; Zok, F. W.; Waite, J. H. Role of transition metals in sclerotization of biological tissue. *Acta Biomater.* **2008**, *4* (6), 2045−2051.

(19) Lee, S. M.; Pippel, E.; Gosele, U.; Dresbach, C.; Qin, Y.; Chandran, C. V.; Brauniger, T.; Hause, G.; Knez, M. Greatly Increased Toughness of Infiltrated Spider Silk. *Science* **2009**, *324* (5926), 488−492.

(20) Dickerson, M. B.; Knight, C. L.; Gupta, M. K.; Luckarift, H. R.; Drummy, L. F.; Jespersen, M. L.; Johnson, G. R.; Naik, R. R. Hybrid fibers containing protein-templated nanomaterials and biologically active components as antibacterial materials. *Mater. Sci. Eng., C* **2011**, *31* (8), 1748−1758.

(21) Li, G. H.; Liu, H.; Zhao, H. S.; Gao, Y. Q.; Wang, J. Y.; Jiang, H. D.; Boughton, R. I. Chemical assembly of TiO2 and TiO2@Ag nanoparticles on silk fiber to produce multifunctional fabrics. *J. Colloid Interface Sci.* **2011**, *358* (1), 307−315.

(22) Mayes, E. L.; Vollrath, F.; Mann, S. Fabrication of magnetic spider silk and other silk-fiber composites using inorganic nanoparticles. *Adv. Mater.* **1998**, *10* (10), 801−805.

(23) Potiyaraj, P.; Kumlangdudsana, P.; Dubas, S. T. Synthesis of silver chloride nanocrystal on silk fibers. *Mater. Lett.* **2007**, *61* (11−12), 2464−2466.

(24) Nisal, A.; Trivedy, K.; Mohammad, H.; Panneri, S.; Sen Gupta, S.; Lele, A.; Manchala, R.; Kumar, N. S.; Gadgil, M.; Khandelwal, H.; More, S.; Laxman, R. S. Uptake of Azo Dyes into Silk Glands for Production of Colored Silk Cocoons Using a Green Feeding Approach. *ACS Sustainable Chem. Eng.* **2014**, *2* (2), 312−317.

(25) Omenetto, F. G.; KapLan, D. L. A new route for silk. *Nat. Photonics* **2008**, *2* (11), 641−643.

(26) Zhang, H.; Zhang, X. T. Modification and Dyeing of Silk Fabric Treated with Tetrabutyl Titanate by Hydrothermal Method. *J. Nat. Fibers* **2014**, *11* (1), 25−38.

(27) Somashekarappa, H.; Annadurai, V.; Sangappa; Subramanya, G.; Somashekar, R. Structure-property relation in varieties of acid dye processed silk fibers. *Mater. Lett.* **2002**, *53* (6), 415−420.

(28) Tansil, N. C.; Li, Y.; Teng, C. P.; Zhang, S. Y.; Win, K. Y.; Chen, X.; Liu, X. Y.; Han, M. Y. Intrinsically Colored and Luminescent Silk. *Adv. Mater.* **2011**, *23* (12), 1463−1466.

(29) Tansil, N. C.; Li, Y.; Koh, L. D.; Peng, T. C.; Win, K. Y.; Liu, X. Y.; Han, M. Y. The use of molecular fluorescent markers to monitor absorption and distribution of xenobiotics in a silkworm model. *Biomaterials* **2011**, *32* (36), 9576−9583.

(30) Tansil, N. C.; Koh, L. D.; Han, M. Y. Functional Silk: Colored and Luminescent. *Adv. Mater.* **2012**, *24* (11), 1388−1397.

(31) Teramoto, H.; Kojima, K. Production of Bombyx mori Silk Fibroin Incorporated with Unnatural Amino Acids. *Biomacromolecules* **2014**, *15* (7), 2682−2690.

(32) Li, B.; Hu, R. P.; Cheng, Z.; Cheng, J.; Xie, Y.; Gui, S. X.; Sun, Q. Q.; Sang, X. Z.; Gong, X. L.; Cui, Y. L.; Shen, W. D.; Hong, F. S. Titanium dioxide nanoparticles relieve biochemical dysfunctions of fifth-instar larvae of silkworms following exposure to phoxim insecticide. *Chemosphere* **2012**, *89* (5), 609−614.

(33) Chen, X.; Shao, Z. Z.; Marinkovic, N. S.; Miller, L. M.; Zhou, P.; Chance, M. R. Conformation transition kinetics of regenerated Bombyx mori silk fibroin membrane monitored by time-resolved FTIR spectroscopy. *Biophys. Chem.* **2001**, *89* (1), 25−34.
(34) Rossle, M.; Panine, P.; Urban, V. S.; Riekel, C. Structural evolution of regenerated silk fibroin under shear: Combined wide- and small-angle x-ray scattering experiments using synchrotron radiation. *Biopolymers* **2004**, *74* (4), 316−327.
(35) Zhou, W.; Chen, X.; Shao, Z. Conformation studies of silk proteins with infrared and Raman spectroscopy. *Prog. Chem.* **2006**, *18* (11), 1514−1522.
(36) Chen, X.; Shao, Z.; Knight, D. P.; Vollrath, F. Conformation transition kinetics of Bombyx mori silk protein. *Proteins: Struct., Funct., Genet.* **2007**, *68* (1), 223−231.
(37) Fossey, S. A.; Tripathy, S. Atomistic modeling of interphases in spider silk fibers. *Int. J. Biol. Macromol.* **1999**, *24* (2−3), 119−125.
(38) Grubb, D. T.; Jelinski, L. W. Fiber morphology of spider silk: The effects of tensile deformation. *Macromolecules* **1997**, *30* (10), 2860−2867.
(39) Plaza, G. R.; Perez-Rigueiro, J.; Riekel, C.; Belen Perea, G.; Agullo-Rueda, F.; Burghammer, M.; Guinea, G. V.; Elices, M. Relationship between microstructure and mechanical properties in spider silk fibers: identification of two regimes in the microstructural changes. *Soft Matter* **2012**, *8* (22), 6015−6026.
(40) Sampath, S.; Isdebski, T.; Jenkins, J. E.; Ayon, J. V.; Henning, R. W.; Orgel, J. P. R. O.; Antipoa, O.; Yarger, J. L. X-ray diffraction study of nanocrystalline and amorphous structure within major and minor ampullate dragline spider silks. *Soft Matter* **2012**, *8* (25), 6713−6722.
(41) Simmons, A. H.; Michal, C. A.; Jelinski, L. W. Molecular orientation and two-component nature of the crystalline fraction of spider dragline silk. *Science* **1996**, *271* (5245), 84−87.
(42) Marsh, R. E.; Corey, R. B.; Pauling, L. An investigation of the structure of silk fibroin. *Biochim. Biophys. Acta* **1955**, *16* (1), 1−34.
(43) Liu, Y.; Yin, L.; Zhao, H.; Song, G.; Tang, F.; Wang, L.; Shao, H.; Zhang, Y. Insights into process-structure-property relationships of poly(ethylene terephthalate) industrial yarns by synchrotron radiation WAXD and SAXS. *J. Appl. Polym. Sci.* **2015**, *132* (36), DOI: 10.1002/app.42512.
(44) Miller, L. D.; Putthanarat, S.; Eby, R. K.; Adams, W. W. Investigation of the nanofibrillar morphology in silk fibers by small angle X-ray scattering and atomic force microscopy. *Int. J. Biol. Macromol.* **1999**, *24* (2−3), 159−165.
(45) Takahashi, Y.; Gehoh, M.; Yuzuriha, K. Structure refinement and diffuse streak scattering of silk (Bombyx mori). *Int. J. Biol. Macromol.* **1999**, *24* (2−3), 127−138.
(46) Martel, A.; Burghammer, M.; Davies, R. J.; Riekel, C. Thermal Behavior of Bombyx mori silk: Evolution of crystalline parameters, molecular structure, and mechanical properties. *Biomacromolecules* **2007**, *8* (11), 3548−3556.

DOI: 10.1021/acssuschemeng.5b00749
ACS Sustainable Chem. Eng. 2015, 3, 2551−2557